27th Symposium on Naval Hydrodynamics
Seoul, Korea, 5-10 October 2008

Comparison Study on Numerical Prediction Techniques for Parametric Roll

Naoya Umeda[1], Hirotada Hashimoto[1], Frederick Stern[2], Shinya Nakamura[1], Seyed Hamid Sadat Hosseini[2], Akihiko Matsuda[3], Pablo Carrica[2],
([1]Osaka University, Japan, [2]The University of Iowa, USA,
[3]National Research Institute of Fisheries Engineering, Japan)

ABSTRACT

For improving prediction capabilities of parametric roll in head waves, a systematic research project, including model experiments, potential flow theory and CFD, is coordinated for a containership. Firstly, captive model tests were executed for measuring roll restoring variation in head waves. Secondly, the Froude-Krylov calculation, potential flow theory and CFD were compared with the measured roll restoring variation. As a result, it was confirmed that the Froude-Krylov calculation underestimates the measured amplitude of restoring variation and the potential flow theory well estimates the amplitude. The CFD overestimates the amplitude of the measured restoring variation but explains the existence of its super-harmonics. Finally, free-running model experiments were conducted and the occurrence and the magnitude of parametric rolling in head waves were provided for validation studies. It was well predicted by a system-based numerical simulation using the potential flow theory for the restoring variation with the coupling effect of surge taken into account.

INTRODUCTION

Parametric roll in longitudinal waves has recently attracted practical attention as a most dangerous phenomenon for large containerships. (France et al., 2003) Once parametric roll starts, the maximum roll angle could reach in excess of 40 to 50 degrees, which is much larger than that due to harmonic resonance in beam seas. Therefore, it is convenient to develop a numerical prediction technique for quantitative parametric roll prediction. Existing analytical or potential theories, however, could be limited in their ability by such extreme situations, such as 50 degrees of roll. To overcome this difficulty, it is desirable to use CFD without rather artificial assumptions. However, because of possible chaotic (Umeda et al., 2004) or non-ergodic (Belenky et al., 2003) behavior due to nonlinearities, numerical simulation should be repeated with a large number of different initial conditions or realizations for a practical stability assessment. Thus, it may be practical to use CFD as an alternative to captive model test for obtaining hydrodynamic forces, particularly restoring variation due to waves. In this context, a combined approach of a system-based simulation dynamics and CFD could be a solution. (Umeda and Hashimoto, 2006)

It is essential to obtain experimental measurements of restoring variation in captive model tests of the containership as the base for validation. Such captive experiments have been often reported in the literature but cases in which both captive and free-running model experiments are available are scarce. In addition, the hull form details used in the experiments are often not available for public release because of commercial reasons. In this project, both free-running and captive model experiments were executed for a containership. In free-running condition the model was exposed to head an following waves. In the captive model experiments, a scaled model of the containership was towed with a heel angle in longitudinal waves and the resulting moment can be regarded as the restoring variation due to waves.

The restoring variation due to longitudinal waves had been theoretically calculated with the Froude-Krylov assumption. (Paulling, 1960) It is often reported that the Froude-Krylov prediction could overestimate the captive model experiment. (Hamamoto and Nomoto, 1982) To improve the agreement between experiments and theory, Boroday (1990) attempted to apply a potential flow theory to a heeled hull so that the restoring moment can be calculated as the sum of the Froude-Krylov, radiation and diffraction components. His numerical results were not comprehensive enough to provide a general conclusion on this issue. Umeda et al. (2005) applied a similar method to containerships and compared with captive model experiments. In this paper, the authors also calculate the radiation and diffraction components of the restoring variation other than the Froude-Krylov component. It is worth noting that if the roll angle is small these components can be regarded as second order components. However, the roll angle cannot be considered small in the case of parametric roll. As an alternative to captive model experiments or potential flow theory, the preliminary use of a RANS equation solver, CFDSHIP-Iowa, is also attempted.

CAPTIVE MODEL EXPERIMENTS FOR MEASURING RESTORING VARIATION

For parametric rolling of the ITTC A-1 containership, which was used for the ITTC benchmark testing study of intact stability in following and stern quartering waves (Umeda and Renilson, 2001), systematic captive tests were carried out at the towing tank of Osaka University which is 100 m in long, 7.8 m in wide and 4.35m in deep. Here its restoring moment in regular head and following waves with a constant heel angle were measured. The results of restoring moment as a function of ship position and wave parameters were provided. Here all data were recorded from the start of the wave maker to the end of model runs for reliable validation of CFD calculation.

Table.1 Principal particulars of the ITTC A-1 Container ship

Items	
length : L_{pp}	150.0m
breadth : B	27.2m
depth : D	13.5m
draught at FP : T_f	8.5m
mean draught : T	8.5m
draught at AP : T_a	8.5m
block coefficient : C_b	0.667
pitch radius of gyration : K_{yy}/L_{pp}	0.25
longitudinal position of centre of gravity from the midship : x_{CG}	1.01m aft
metacentric height : GM	1.0m
natural roll period : T_ϕ	20.1s
rudder area : A_R	28.11m^2
propeller diameter : D_p	5.04m

A 1/60 scaled model of the ITTC A-1 containership was used; its principal dimensions and body plans are shown in Table 1 and Fig. 1, respectively. The model was free in heave and pitch, and was attached to a towing carriage with a dynamometer. Then it was towed by the carriage in regular head and following waves. The resulting surge force, sway force, roll moment and yaw moment were measured by the dynamometer and the heave and the pitch motions were measured by potentiometers. The water waves were generated by a plunger type wave maker and the water elevation were detected by a servo-needle wave height meter attached to the towing carriage.

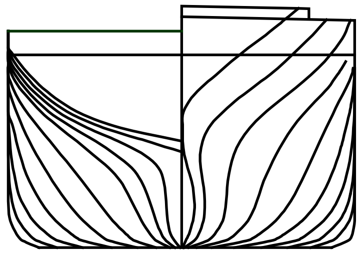

Fig.1 Body plan of the ITTC A-1 Container ship

In the head-sea experiment, the wave length to ship length ratios, λ/L_{pp}, were 1.0, 1.25 and 1.5, the wave steepness, H/λ, were 0.01, 0.02, 0.03 and 0.04 and the Froude number, F_n, were 0.05, 0.1, 0.15 and 0.2. In the following-sea experiment, the wave length to ship length ratios were 1.0, 1.25 and 1.5, the wave steepness were 0.03, 0.04, 0.05 and 0.06 and the Froude number were 0.15, 0.2, 0.25 and 0.3.

The model runs were executed with the upright condition and the condition with the heel angle, ϕ, of 10 degrees so that the metacentric height, GM, were estimated with the difference in the roll moments between the two conditions, K.

$$GM = -\frac{K}{W \sin\phi} \tag{1}$$

where W is the ship weight. Then the mean, the amplitudes of its first and second harmonic components and their phase lag from the waves were calculated from the records as functions of the relative position of the center of ship gravity to the wave length as follows (Nakamura et al., 2007):

$$\begin{aligned} GM &= a + b_1 \cos\{2\pi(\xi_G / \lambda - \varepsilon_1)\} \\ &\quad + b_2 \cos\{4\pi(\xi_G / \lambda - \varepsilon_2)\} \end{aligned} \tag{2}$$

Here the ratio of the horizontal distance of the center of ship gravity from a wave trough to the wave length is denoted as ξ_G/λ.

The experimental results are shown in Figs. 2-10 as functions of the wave steepness. The mean of the restoring variation due to waves is roughly proportional to the square of the wave steepness, while the amplitude of the first harmonic component of the restoring variation due to waves is roughly proportional to the wave steepness. The first harmonic component of the metacentric height variation increases with increasing wave length and decreases with increasing forward velocity. The second harmonic component is comparable to the first harmonic component, and increases with increasing wave steepness.

PREDICTION OF RESTORING VARIATION WITH POTENTIAL FLOW THEORY

It is desirable for theoretically estimating the restoring variation due to waves. Thus, two methods are applied in this paper: one is the Froude-Krylov prediction and the other is the application of a strip theory including radiation and diffraction components. The Froude-Krylov component is calculated by integrating the incident wave pressure around the instantaneous wetted hull surface. Since the incident wave pressure changes as an exponential function of the water depth, it was represented by the local ship draught. The heave and pitch motions, to be used for determining the instantaneous wetted surface, are estimated by a linear strip theory for an upright hull. As a result, the obtained Froude-Krylov component of the restoring variation depends on the ship forward velocity, and has nonlinear relationship with the wave steepness.

If we apply a strip theory to a heeled hull, other than the Froude-Krylov component, roll radiation moment due to vertical motions and roll diffraction moment can be calculated. This is because an asymmetric section form results in hydrodynamic coupling from heave to roll within a 2D plane. In this paper, these 2D hydrodynamic coefficients are calculated by numerically solving an integral equation of the velocity potential of potential flow around the cross section. Then, following the framework of a strip theory, roll radiation and diffraction moments are calculated with the assumption of small amplitude waves and the resulting ship motions. Here so-called “end terms” are included so that hydrodynamic lift components are also taken into account within the framework of a linear slender wing theory. These additional hydrodynamic components have linear relationships with the wave steepness. Thus, the restoring variation estimated here consists of the nonlinear Froude-Krylov component and the linear radiation and diffraction components.

The calculated results using these two methods are also plotted in Figs. 2-10, if applicable. Since the strip theory used here only deal with the leading terms, the mean and the second harmonic components cannot be calculated. Regarding the mean value, Ogawa and Ishida (2006) presented a prediction theory and obtained good agreements with the captive model experiment of a post-Panamax containership at least at low speed.

If we take account of the radiation and diffraction components, the amplitude of the first harmonic component of the metacentric height variation generally increases. When the wave length is longer than the ship length, however, the effect of radiation and diffraction becomes smaller at least smaller wave steepness.

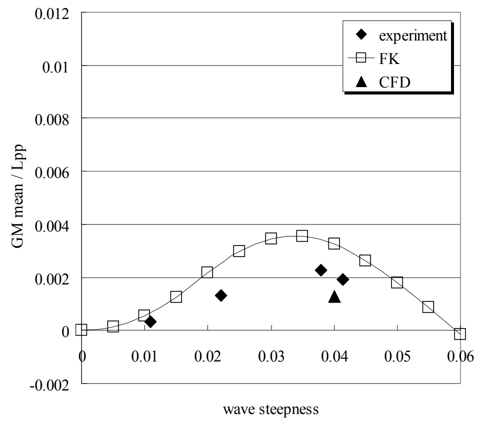

Fig.2 Mean of the metacentric height variation with λ / L_{PP} =1.0 and Fn = 0.1 in head seas

The measured mean of the metacentric height variation is qualitatively explained by the Froude-Krylov prediction. It is noteworthy here that the mean value initially increases with the increasing wave steepness and then decreases with the wave steepness. The measured first harmonic component of the metacentric height variation is well explained by the Froude-Krylov component for the subject containership. This result is different from a post-Panamax containership investigated before (Umeda and Hashimoto, 2006), as shown in Figs. 11-12. The measured second harmonic component of the metacentric variation is roughly evaluated by the Froude-Krylov prediction but the tendency is not so well reproduced.

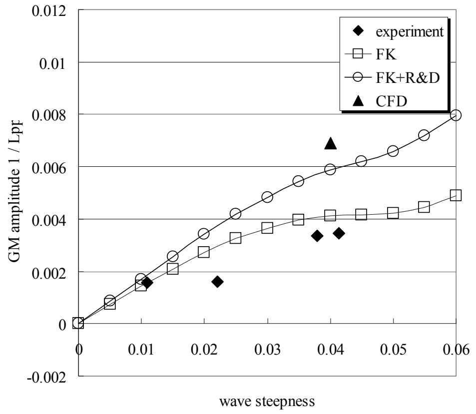

Fig.3 Amplitude of the first harmonic component of metacentric height variation with λ / L_{PP} =1.0 and Fn=0.1 in head seas

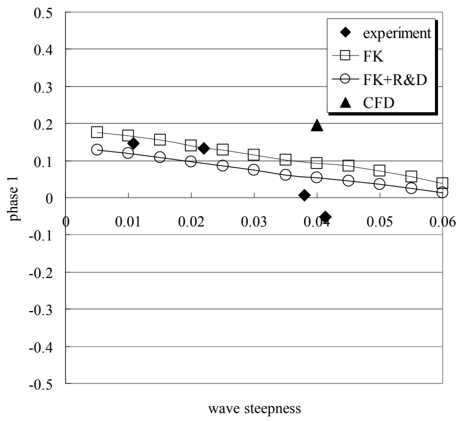

Fig.4 Phase of the first harmonic metacentric height variation with λ / L_{PP} =1.0 and Fn=0.1 in head seas

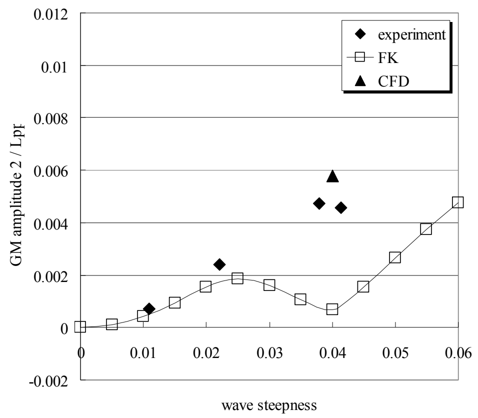

Fig.5 Amplitude of the second harmonic component of metacentric height variation with λ / L_{PP} =1.0 and Fn=0.1 in head seas

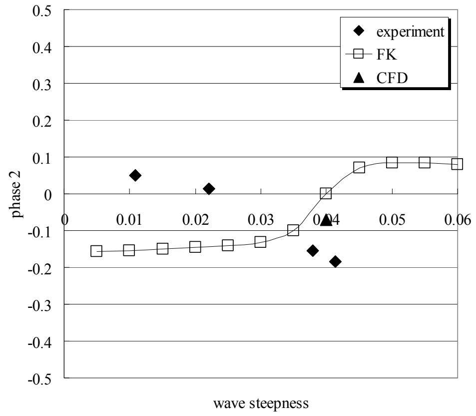

Fig.6 Phase of the second harmonic component of metacentric height variation with λ / L_{PP} =1.0 and Fn=0.1 in head seas

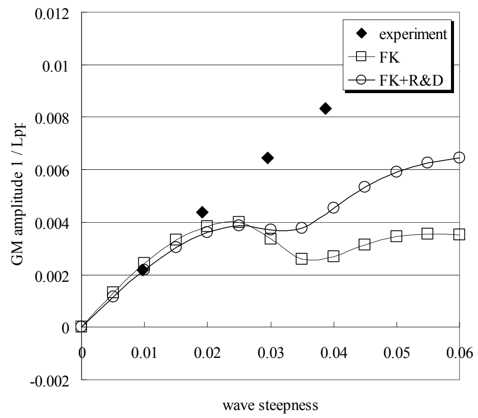

Fig.7 Amplitude of the first harmonic component of metacentric height variation with λ / L_{PP} =1.25 and Fn=0.1 in head seas

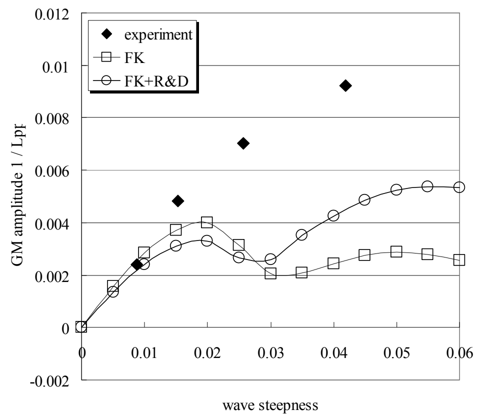

Fig.8 Amplitude of the first harmonic component of metacentric height variation with λ / L_{PP} =1.5 and Fn=0.1 in head seas

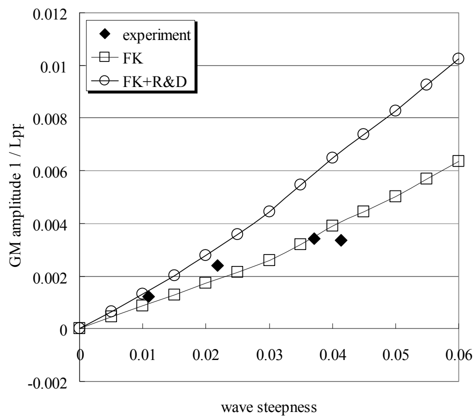

Fig.9 Amplitude of the first harmonic component of metacentric height variation with λ / L_{PP} =1.0 and *Fn*=0.15 in head seas

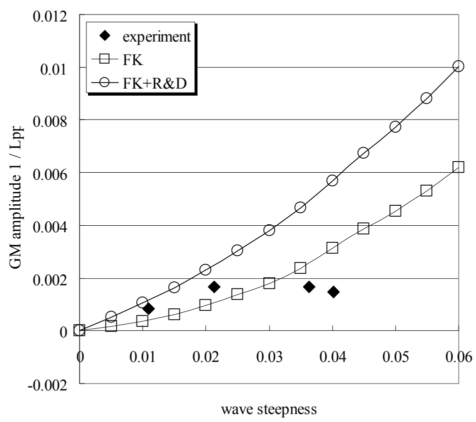

Fig.10 Amplitude of the first harmonic component of metacentric height variation with λ / L_{PP} =1.0 and *Fn*=0.2 in head seas

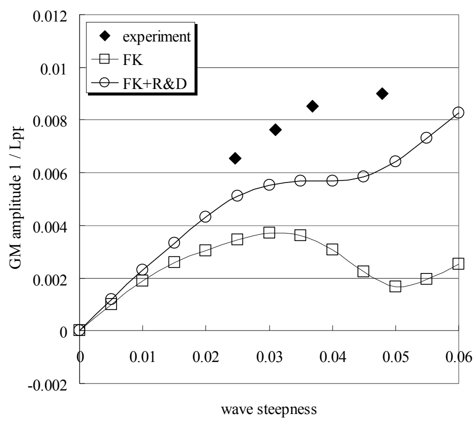

Fig.11 Amplitude of the first harmonic component of metacentric height variation with λ / L_{PP} =1.0 and *Fn*=0.1 in head seas for the post-Panamax containership

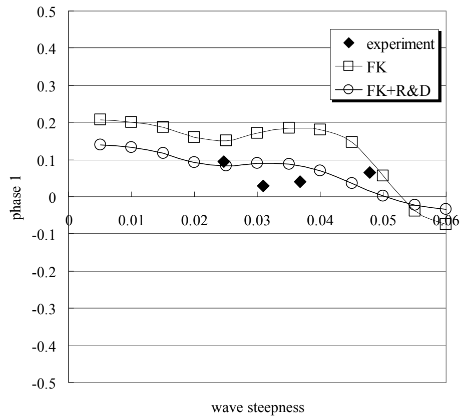

Fig.12 Phase of the first harmonic component of metacentric height variation with λ / L_{PP} =1.0 and *Fn*=0.1 in head seas for the post-Panamax containership.

CFD CALCULATION

To realise more direct and accurate estimation of roll restoring variation for parametric roll prediction, the single-phase level-set code CFDSHIP-Iowa version 4 (Carrica, et al., 2006) is applied for this problem and the results compared with experiments and calculations based on the potential flow theory. Recently validation efforts of the CFDSHIP-Iowa for heave and pitch motions in regular waves (Carrica et al., 2007b), parametric rolling (Stern and Campana, 2008), broaching (Carrica, et al., 2007a) are available in the literature. If the capability of the code for hydrodynamic force estimation in waves is confirmed, advanced numerical prediction technique with the combination of system-based simulation and CFD becomes a powerful tool for stability assessment in waves. CFDSHIP-Iowa is a single-phase code, thus the effects of air are ignored. CFDSHIP-Iowa solves the RANS equations using a blended k-ω/k-ε model for the turbulence. The free surface is modeled using a level set approach, in which the air/water interface is the zero level set distance function. The domain is discretized using multiblock/overset structured grids. The capability of the overset is fully dynamic, which allows simulating large amplitude motions in waves. Numerical methods include a finite differences discretization, with second-order upwind discretization of the convection terms and second-order cantered scheme for the viscous terms. The temporal terms are discretized using a second-order backwards Euler scheme. Incompressibility is enforced by a strong pressure/velocity coupling by using PISO. Regular waves are implemented through initial and boundary conditions. The fluid flow equations are solved in an earth-fixed inertial reference system, while the rigid body equations are done in the ship system, therefore forces and moments are projected appropriately to perform the integration of the rigid body equations of motion, which are solved iteratively. The overset connectivity can be obtained using the code Suggar (Noack, 2005).

Geometry with hull surface grid of the subject ship is shown in Fig.13. Bow flare and stern deck are included for accurate capturing the change of secondary moment of the water plane due to wave elevation in steep waves. The overset grid design consists of 4 grids as shown in Fig.14. Two double-O boundary layer grids model the starboard and port sides of the hull to solve the asymmetric problem due to heel. Two Cartesian grids are used as refinement and background for the fluid flow and free surface, and these grids are not subject to heave and pitch motions. Although the subject ship has bilge keels, there is no grid for bilge keels because their effect on roll restoring variation for constant heeling condition is assumed to be negligibly small. In Table.2 the grid sizes of each grid block are shown.

The CFD calculation is executed for the case of the metacentric height variation with the wave length to ship length ratio of 1.0, the wave steepness of 0.04 and the Froude number of 0.1 in head seas. The obtained result is expanded in a form of Equation (2) and the coefficients are plotted in Figs. 2-6. The CFD underestimates the mean of the restoring variation and overestimates the amplitude of the first harmonic component. It should be noted that the CFD very well estimates the second harmonic component both in amplitude and the phase lag, while the linear potential flow theory is not useful for this component. The CFD result is presented as a function of the relative ship position to a wave trough in Fig. 15 together with the captive model test, the Froude-Krylov prediction and the strip theory including radiation and diffraction components. This can be regarded as a time history because the model is towed with a constant velocity.

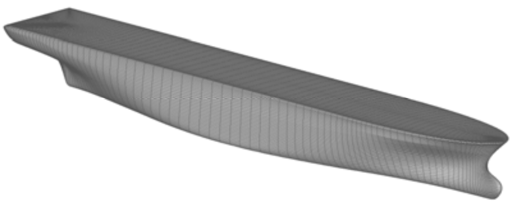

Fig.13 Geometry of the subject ship

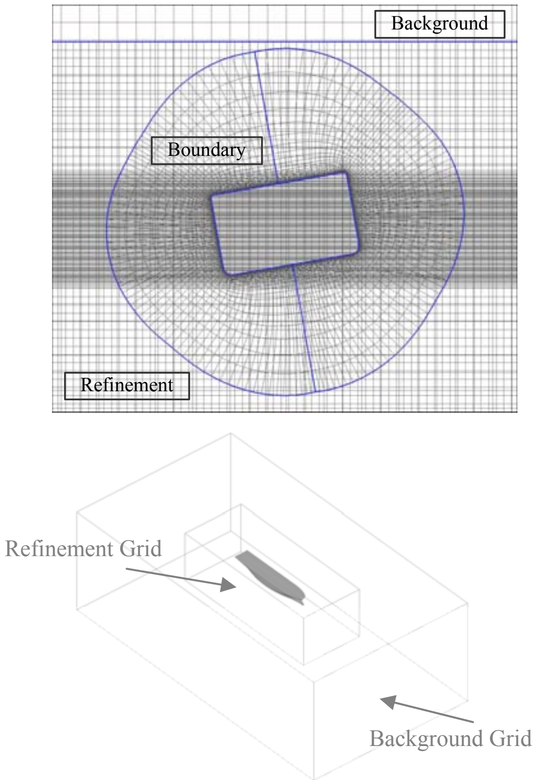

Fig.14 Overset grids

Table 2 Grid size

Grid	Points
Boundary –Starboard	377,010
Boundary –Port	377,010
Refinement	1,352,000
Background	1,455,300
Total	3,561,320

The metacentric height variation measured in the experiment consists of mainly the harmonic component and the super-harmonic (2^{nd} harmonic) component. Here the zero value is set to be equal to its calm-water value. When the ship center exists at the wave down slope near a wave crest, the metacentric height becomes the minimum. When the ship center exists in the wave down slope near a wave trough, the metacentric height becomes the maximum. When the ship center exists in the wave up slope, the metacentric height is generally larger than its calm-water value. The Froude-Krylov prediction well explains this qualitative nature but the predicted amplitude is smaller than the measured one. The strip theory including radiation and diffraction components provides a better agreement with the experiment but does not clearly explain the secondary peak in the wave up slope. The CFD well explains the secondary peak in the wave up slope but significantly underestimates the minimum value near a wave crest. Thus it can be stated that the current CFD qualitatively explains the experiment but not quantitatively. The comparisons in heave and pitch motions between the experiment and the CFD are also shown in Figs. 16-17. The CFD overestimates the measured heave amplitude and underestimates the measured pitch amplitude. Further improvement of the CFD computation such as grid study, thus, could be required. Fig.18 shows the instantaneous free surface and ship attitude computed by the CFD. The bulbous bow is out of the water when the ship center is located around a wave up slope, and the bow almost submerges when the ship center is on a wave trough.

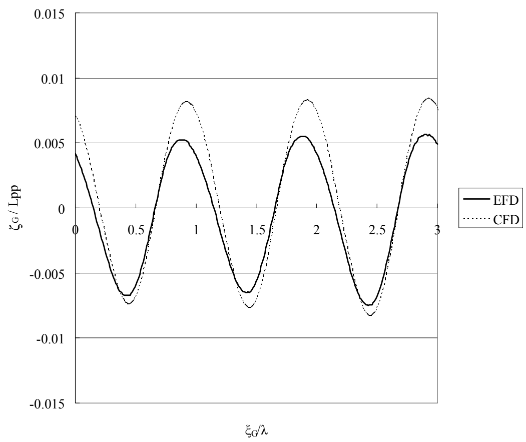

Fig. 16 Comparison in the time series of heave displacment among the experiment and the CFD with λ/L_{pp}=1.0, H/λ=0.04 and Fn= 0.1 in head seas.

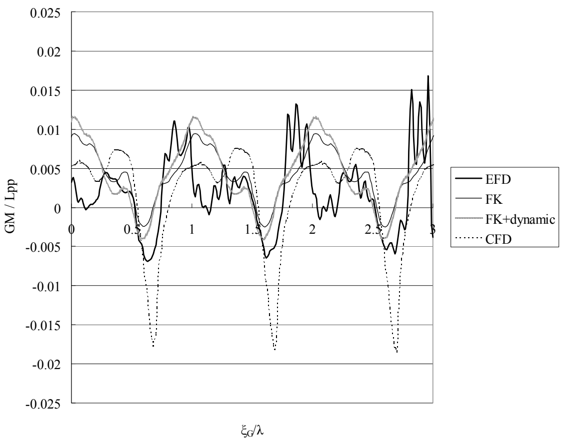

Fig. 15 Comparison in the time series of metacentric height variation among the experiment, the Froude-Krylov prediction, the strip theory including the Froude-Krylov, radiation and diffraction components and the CFD with λ/L_{pp}=1.0, H/λ=0.04 and Fn= 0.1 in head seas.

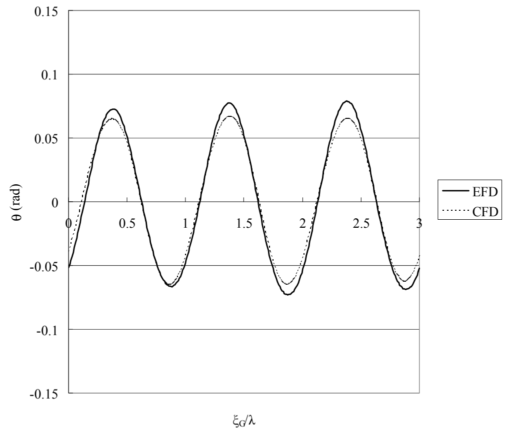

Fig. 17 Comparison in the time series of pitch angle among the experiment and the CFD with λ/L_{pp}=1.0, H/λ=0.04 and Fn= 0.1 in head seas.

The CFD is applied also to the case of Fn=0.2 as shown in Fig. 19. At this Froude number in the model experiment, secondary peaks of the metacentric height variation becomes comparable to major peaks. The CFD well reproduces secondary peaks while the potential flow theory cannot do. And the CFD well predicts the double amplitude of the metacentric height variation. This means that the CFD provides better agreements with the experiment at higher speed region.

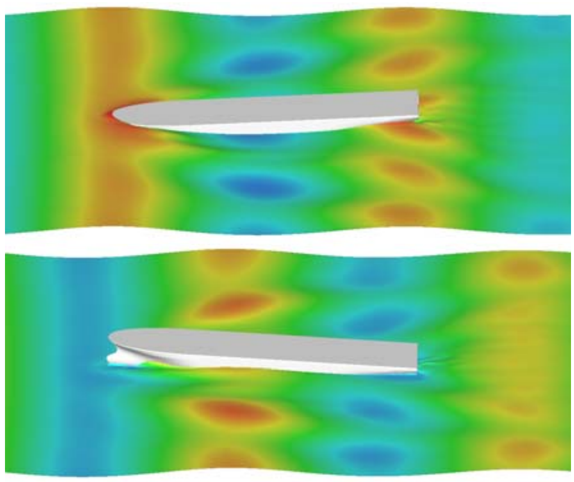

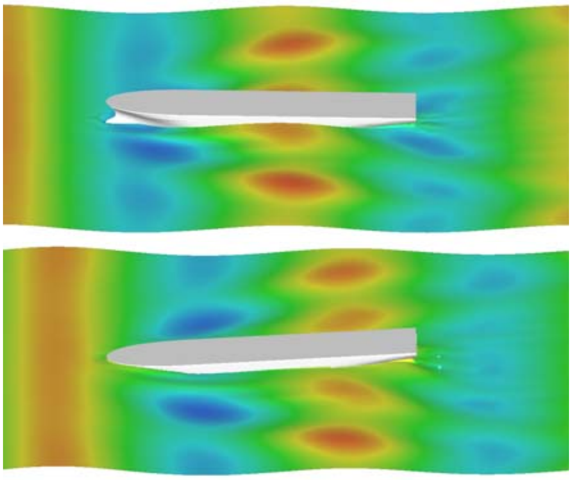

Fig. 18 Bird's-eye views of the ship and wave behavior obtained by CFD with λ/L_{pp}=1.0, H/λ=0.04 and Fn= 0.1in head seas. (From top: trough, up-slope, crest, down-slope)

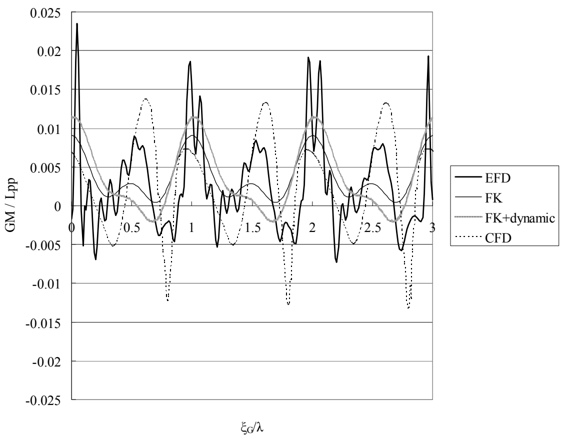

Fig. 19 Comparison in the time series of metacentric height variation among the experiment, the Froude-Krylov prediction, the strip theory including the Froude-Krylov, radiation and diffraction components and the CFD with λ/L_{pp}=1.0, H/λ=0.04 and Fn= 0.2 in head seas.

FREE-RUNNING MODEL EXPERIMENT

The free-running model experiment was conducted at the seakeeping and maneuvering basin of National Research Institute of Fisheries Engineering, which is 60 meters in long, 25 meters in wide, 3.2 meters in deep and has an 80 segmented plunger-type wave maker. The model used was equipped with a electric motor, a steering gear, an onboard computer and a fiber optical gyroscope. The model was propelled by the electric motor with a constant revolution control system and was steered to keep a specified straight course by utilizing an autopilot with the rudder gain of 1. The roll angle, pitch angle and yaw angles were detected by the gyroscope. The horizontal position relative to the basin was measured by an optical tracking system with a CCD camera attached to the cat walk of the basin roof. The GZ curve from hydrostatics and the roll extinction curve from a roll decay test without forward velocity are shown in Figs. 20 and 21, respectively.

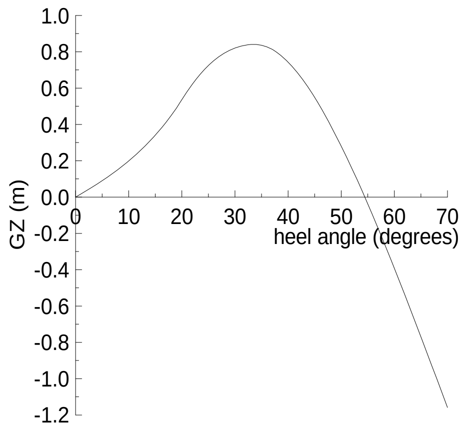

Fig. 20 Restoring arm curve of the tested containership.

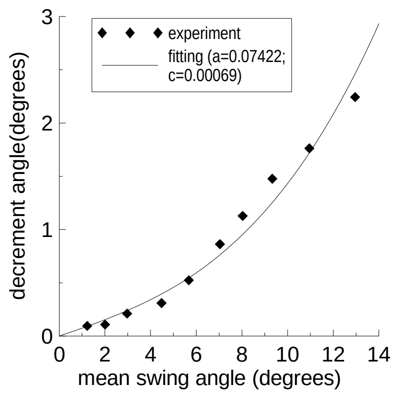

Fig. 21 Roll extinction curve of the tested containership model without forward velocity. Here a and c indicate linear and cubic coefficients, respectively.

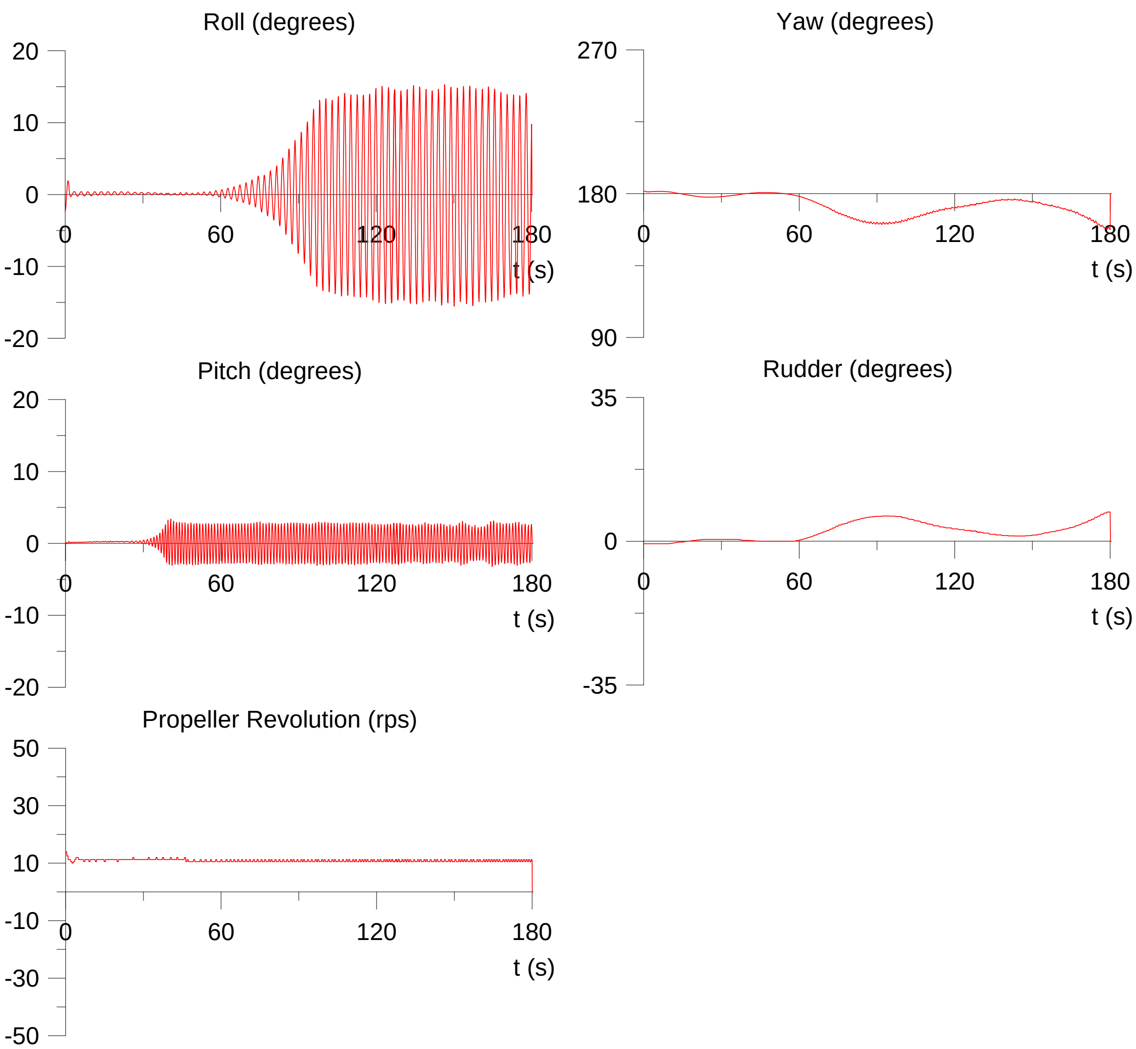

Fig. 22 An example of time records of head-sea parametric rolling of the containership model in the free-running test. Here the wave steepness of 0.03, the wave length to ship length ratio of 1.25 and the nominal Froude umber of 0.1.

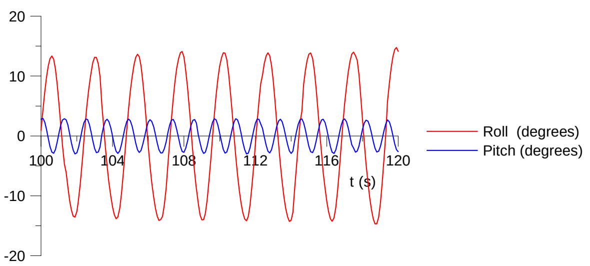

Fig. 23 Enlargement of the time series of the roll and pitch motions shown in Fig. 22.

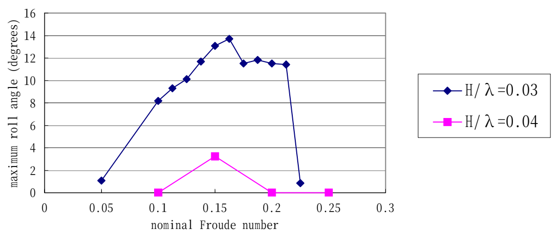

Fig.24 Measured maximum roll angle on parametric roll with λ/L_{PP} =1.0

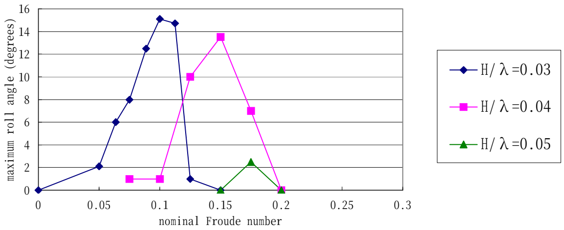

Fig.25 Measured maximum roll angle on parametric roll with λ/L_{PP} =1.25.

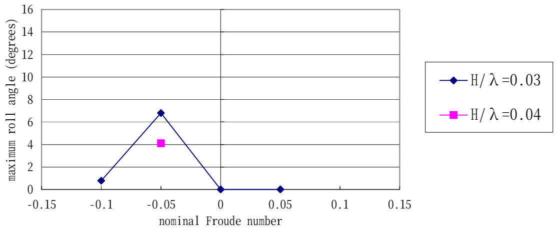

Fig.26 Measured maximum roll angle on parametric roll with λ/L_{PP} =0.8.

An example of the model run in head waves is shown in Fig. 22. Here the wave-length to ship length ratio is 1.25 and the wave steepness is 0.03. The nominal Froude number, which corresponds to the calm-water velocity with the same propeller revolution, is 0.1. The model firstly ran in calm water with the constant propeller revolution and then met a regular wave train from the bow. The pitch motion was excited by the regular wave train and it was quickly settled into a periodic state. At the same time the roll motion started to gradually increase. After t=60 seconds, this increase became significant. And then an almost periodic state appeared. It is noteworthy that after t=60 seconds a small yaw motion with very low frequency and small deviation from the specified course were observed. Because of the auto pilot, the rudder deflection also occurred. This is probably because the feedback system of the ship-autopilot has a natural frequency and some disturbance from the roll motion is given. If we enlarge the time series of the roll and pitch, as shown in Fig. 23, the roll period was twice as large as the pitch period, and is almost equal to the natural roll period. Therefore, this is parametric rolling in head waves. The amplitude of the roll was about 14 degrees. Because of low frequency yaw motion, the roll motion envelope also had a low frequency fluctuation.

The model runs were carried out in regular head waves and regular following waves for the several Froude numbers. The wave length to ship length ratio ranges from 0.8 to 1.25 and the wave steepness ranges from 0.03 to 0.05.The results are shown in Figs. 24-26. The abscissa indicates the nominal Froude number. Here the positive nominal Froude number means head waves and the negative does following waves. In case of head waves, the actual Froude number could be smaller than the nominal one because of added resistance due to waves. The ordinate indicates the maximum roll angle during the model runs. Because of a small yaw motion with very low frequency, it is not always possible to identify steady roll motions in the model runs.

Parametric rolling could occur only in the limited speed range. In case of the wave steepness of 0.03, when the Froude number increases the amplitude of parametric rolling gradually increases. On the contrary, when the Froude number further increases the amplitude of parametric rolling suddenly decreases. This qualitative difference can be explained with the bifurcation theory: the former case is known as the super critical bifurcation and the latter is as the sub-critical bifurcation. This is the results of nonlinearity of restoring moment at large heel angle.

When the wave steepness increases, the parametric rolling becomes smaller and then disappears. This can be explained as follows. The mean of the metacentric height variation increases with increasing the wave steepness as shown in Fig. 2 so that the effective natural frequency increases for larger wave steepness. As a result, the condition of parametric rolling is shifted to higher Froude number. Since the roll damping increases due to higher Froude number, parametric rolling could disappear.

SYSTM-BASED PREDICTION OF PARA-METRIC ROLL

For predicting parametric rolling, Umeda et al. (2005) and Hashimoto et al. (2007) developed a numerical model in the time domain as follows:

$$\ddot{\phi} + 2\alpha\dot{\phi} + \gamma\dot{\phi}^3 + \frac{W}{(I_{xx} + J_{xx})} GZ(t, \zeta_G, \theta, \phi) = 0 \qquad (3)$$

where ϕ: roll angle, I_{xx}: moment inertia of ship in roll, J_{xx}: added moment of inertia in roll, α: linear roll damping coefficient, γ: cubic roll damping coefficient. W: ship weight, GZ: restoring arm, t: time, ζ_G: heave displacement and θ: pitch angle. This model has a single degrees of freedom but coupling in restoring term from heave and pitch to roll is taken into account. The heave and pitch motion is linearly estimated in advance and used for the input to the above model. The roll restoring variation is calculated with the strip theory including radiation, diffraction and nonlinear Froude-Krylov prediction. The roll damping coefficients are estimated with roll decay test results of the scaled ship model. In this paper, the above model is called as "1 DOF model". This model was applied to a post-Panamax containership and a car carrier and slightly overestimates the amplitude of parametric rolling in model experiments.

To improve prediction accuracy, the authors newly take the coupling effect with surge into account. This is because the surging motion could modulate periodic restoring variation so that parametric rolling to some extent could be deteriorated. The surge equation to be added is as follows:

$$(m+m_x)\ddot{X}_G = T(\dot{X}_G, n) - R(\dot{X}_G) + F_X(X_G, t) - R_w(\dot{X}_G, t) \quad (4)$$

where X_G: instantaneous ship longitudinal position, m: ship mass, m_x: added mass in surge, T: propeller thrust, n: propeller rate, R: ship calm-water resistance, F_X: wave-induced surge force and R_W: added resistance due to wave. Here the propeller thrust and calm-water resistance are estimated with a propeller open test result and a resistance test in calm-water, respectively. The wave-induced surge force is linearly calculated with the Froude-Krylov assumption. The added resistance is estimated with Maruo's theory (Maruo, 1960) and the Kochin function estimated by Kashiwagi's slender body theory (Kashiwagi, 1995, 1997). The obtained surge displacement is utilized to determine the roll restoring variation as a function of relative position of the ship to waves. Thus, if the ship speed is fluctuated, the restoring variation could be modulated. In this paper, this method is called as "2 DOF model".

Numerical results with both the 1 DOF and 2 DOF models are compared with the free-running model experiments as shown in Figs. 27-28. In Fig. 27, the amplitudes of the parametric rolling are indicated as functions of the nominal Froude number. The 1 DOF model overestimates the amplitude of parametric rolling and the estimated occurrence zone is shifted. On the contrast, the 2 DOF model provides satisfactory agreements in the amplitude and the occurrence zone of parametric rolling with the free-running model experiments. In Fig. 28, the amplitudes are plotted as functions of the actual Froude number, which was measured by an optical tracking system during the experiment. The forward speed estimated by the 2 DOF model well agrees with the measured forward speed. The estimated amplitude also agrees with the measure one. This indicates that prediction of speed loss in head waves is satisfactory and the effect of the forward velocity on parametric rolling is accurately evaluated. The fact that the amplitude from the 2 DOF model is smaller than that from the 1 DOF model and agrees with the experiment supports authors' hypothesis that the surge-induced modulation could reduce the amplitude of parametric rolling. Therefore, the coupling with the surge motion is essential for accurately predicting parametric rolling in head waves.

A future task could be a comparison in parametric roll amplitude between the system-based prediction and the CFD-based prediction. Although Fred and Campana (2008) already presented a promising comparison on parametric rolling of the ONR tumblehome vessel, it could be a still challenge because good prediction of restoring variation at low speed is required here.

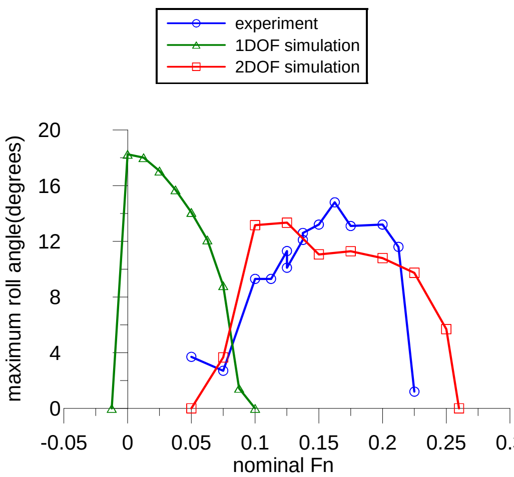

Fig. 27 Comparison in parametric roll amplitude as functions of the nominal Froude number among 1 DOF model, the 2 DOF model and the experiment with λ/L_{pp}=1.25 and H/λ=0.03.

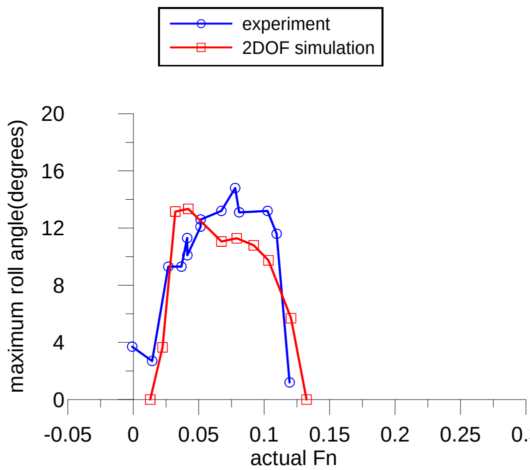

Fig. 28 Comparison in parametric roll amplitude as functions of the actual Froude number between the 2 DOF model and the experiment with λ/L_{pp}=1.25 and H/λ=0.03.

CONCLUDING REMARKS

The experimental data of metacentric height variation for a containership in head waves are provided for the validation of hydrodynamic tools. Current comparison shows that the strip theory including radiation and diffraction and nonlinear Froude-Krylov component provides acceptable agreements with the experiment and the even nonlinear Froude-Krylov component on its own is sufficient for longer waves. The CFD currently overestimates the amplitude of the measured metacentric height variation at low speed but well explains the existence of secondary peak due to its super-harmonics.

The experimental data of parametric rolling for the containership in head waves are provided for the validation of numerical tools for head-sea parametric rolling. It was confirmed that a system-based simulation using the strip theory for the restoring variation reasonably well predict the occurrence and magnitude of parametric rolling in regular head waves if the coupling effect of surge is taken into account.

ACKNOWLEDGEMENTS

The work was supported by the US Office of Naval Research Contract No. 0014-06-1-0646 under the administration of Dr. Patrick Purtell, and by a Grant-in Aid for Scientific Research of the Japan Society for Promotion of Science (No. 18360415) The authors express their sincere gratitude to the above organizations. The authors thank Prof. S. Naito for allowing them to use his computer program on added resistance in waves for this study. In addition, the assistance during the experiments from Misses. E. Maeda and I. Tsukamoto and Mr. A. Maki is also acknowledged.

REFERENCES

Belenky, V., Weems, K.M., Lin, W.M. and Paulling, J.R., "Probabilistic Analysis of Roll Parametric Resonance in Head Seas", Proceedings of the 8th International Conference on Stability of Ships and Ocean Vehicles, Universidad Politecnica de Madrid, 2003, pp.325-340

Boroday, I.K., "Ship Stability in Waves: On the Problem of Righting Moment Estimations for Ships in Oblique Waves", Proceedings of the 4th International Conference on Stability of Ships and Ocean Vehicles, Federico II University, 1990, pp.441-451

Carrica, P.M., Wilson, R.V., Noack, R., Xing, T., Kandasamy, M., Shao, J., Sakamoto, N., and Stern, F., "A Dynamic Overset, Single-phase Level Set Approach for Viscous Ship Flows and Large Amplitude Motions and Maneuvering", Proceedings of the 26th Symposium on Naval Hydrodynamics, ONR, 2006, CD.

Carrica, P.M., Paik, K.J., and Stern, F., "URANS Analysis of a Broaching Event in Irregular Quartering Seas", Proceedings of International Conference on Violent Flows, Kyushu University, 2007a, CD.

Carrica, P.M., Wilson, R.V., and Stern, F., "Ship Motions Using Single-Phase Level Set with Dynamic Overset Grids", Comput. Fluids, Vol. 36, 2007b, pp.1415-1433.

France, W.L. et al., "An Investigation of Head-Sea Parametric Rolling and Its Influence on Container Lashing Systems", Marine Technology, 40(1), 2003.

Hamamoto, M. and Nomoto, K., "Transverse Stability of Ships in a Following Sea", Proceedings of the 2nd International Conference on Stability of Ships and Ocean Vehicles, Society of Naval Architects of Japan, 1982, pp. 215-224.

Hashimoto, H., Umeda, N. and Sakamoto, G., "Head-Sea Parametric Rolling of a Car Carrier", Proceedings of the 9th International Ship Stability Workshop, Germanscher Lloyd, 2007, pp.4.5.1-4.5.7

Kashiwagi, M., "Prediction of Surge and Its Effect on Added Resistance by Means of the Enhanced Unified Theory", Trans. of West-Japan Soc. Nav. Arch.,No.89, 1995, pp.77-89.

Kashiwagi, M., "Numerical Seakeeping Calculations Based on the Slender Ship Theory", Schiffstechnik, Vol.4, No.4, 1997, pp.167-192.

Maruo, H., "Wave Resistance of a Ship in Regular Head Seas", Bulletin of the Faculty of Eng., Yokohama National Univ., Vol.9, 1960, pp.73-91.

Nakamura, S., Umeda, N., Hashimoto, H. and Sakamoto, G., "Hull Form Effect on Restoring Variation of Containerships in Head Seas", Conference Proceedings of the Japan Society of Naval Architects and Ocean Engineers, Vol.5E, 2007, pp.33-36, (in Japanese)

Noack, R., "SUGGAR: a general capability for moving body overset grid assembly" Proceedings of the 17th

AIAA Computational Fluid Dynamics Conference, 2005.

Ogawa, Y. and Ishida, S., "The Analytical Examination of the Righting Moment Variation in Waves", Conference Proceedings of the Japan Society of Naval Architects and Ocean Engineers, Vol.2K, 2006, pp.17-18, (in Japanese)

Paulling, J.R., "Transverse Stability of Tuna Clippers", Fishing Boat of the World, Vol.2, edited by J.O. Traung, Fishing News Limited, 1960, pp.489-495

Stern, F. and Campana, E., "Head-Waves Parametric Rolling of Surface Combatant," Proceedings of the Symposium on Limit Cycle Oscillation and Other Amplitude-Limited Self-Excited Vibrations, AVT-152, Loen, Norway, 2008.

Umeda, N., Hashimoto, H., Vassalos, D., Urano, S. and Okou, K., "Nonlinear Dynamics on a Parametric Roll Resonance with Realistic Numerical Modelling", International Shipbuilding Progress, Vol.51, No.2/3, 2004, pp.205-220

Umeda, N. and Renilson, M.R., "Benchmark Testing of Numerical Prediction on Capsizing of Intact Ships in Following and Quartering Seas", Proceedings of the 5th International Workshop on Stability and Operational Safety of Ships, University of Trieste, 2001, pp.6.1.1-6.1.10

Umeda, N., Hashimoto, H., Sakamoto, G. and Urano, S., "Research on Roll Restoring Variation in Waves", Conference Proceedings of the Kansai Society of Naval Architects, Vol.24, 2005, pp.17-19, (in Japanese)

Umeda, N. and Hashimoto, H., "Recent developments of capsizing prediction techniques of intact ships running in waves", Proceedings of the 26th Symposium on Naval Hydrodynamics, ONR, 2006, CD.